Fischer Tropsch synthesis using Co based carbon catalysts

Sarwat Iqbal[a], Thomas E. Davies[b], David J. Morgan[a], Khalid Karim[c], James S. Hayward[a], Jonathan K. Bartley [a], Stuart H. Taylor[a], and Graham J. Hutchings[a,]*

*hutch@cardiff.ac.uk

[a] Cardiff Catalysis Institute, School of Chemistry, Cardiff University, Main Building, Park Place, Cardiff UK CF10 3AT

[b] Stephenson Institute for Renewable Energy, Chemistry Department, The University of Liverpool, Crown Street, Liverpool, UK, L69 7ZD

[c] SABIC T&I, P.O Box 42503, Riyadh 11551, Saudi Arabia

Abstract

The catalytic activity of a series of carbon-supported cobalt manganese oxide ($CoMnO_x$) catalysts was investigated for the Fischer Tropsch synthesis reaction. The catalysts were compared with an unsupported $CoMnO_x$ catalyst under the same reaction conditions, and it was shown that the use of an activated carbon support increased both the catalyst activity and the selectivity to C_{2+} hydrocarbons, whilst lowering the selectivity to CH_4 and CO_2. Additionally, the effects of varying heat treatment temperatures and increasing the precursor ageing times were also investigated. Increasing the heat treatment temperature of the catalyst precursor between 300 and 500 °C led to an increase in activity, as well as an increase in selectivity to C_{2+} hydrocarbons, but it also increased the selectivity to CO_2. At 600 °C there was a marked decrease in activity, and the main product was C_{5+} hydrocarbons. Ageing the initial precipitate led to a decrease in activity and also decreased the selectivity towards hydrocarbons.

Keywords: Fischer Tropsch synthesis, syngas, carbon support, cobalt, cobalt manganese catalysts

1. Introduction

Fischer Tropsch synthesis (FTS) is valuable for the production of clean liquid fuels from syngas (CO + H_2). The product distribution in FTS is, however, typically very broad and a major part of the extensive current research is focussed on controlling the selectivity to the desired products. Fe, Co, and Ru are active catalysts for FTS, but only Fe and Co are used extensively. Although ruthenium exhibits excellent activity for this reaction, its limited availability and cost prohibits its use on an industrial scale. Iron based catalysts have been shown to be active for the formation of hydrocarbons at higher reaction temperatures, but suffer from complex phase formation and deactivation by water. Cobalt catalysts are active at lower temperatures than Fe and tend to produce light hydrocarbons, particularly when promoted with manganese oxide. A range of studies have been published on $CoMnO_x$ catalysts for the synthesis of light hydrocarbons, and they demonstrate lower selectivity to methane [1-8]. It has been observed that Co in combination with manganese oxide can produce high yields of alkenes with increasing CO conversion, whereas this is not observed with cobalt only catalysts [3]. The use of partially reducible oxides such as MnO_2 [7], and TiO_2 [9] has been shown to improve the selectivity towards light alkenes in FTS using cobalt as the active metal component.

It is well-established that the catalytic activity depends on the number of surface metal sites available for reaction. A common method of increasing the dispersion and stability of metal is supporting the particles on a stable metal oxide, such as Al_2O_3 or SiO_2. However, it has been observed that the strong metal-support interaction can lead to the formation of undesirable phases such as $CoAl_2O_4$, and these mixed oxides are believed to be a cause of deactivation that is generally observed with these catalysts. The utilization of inert supports can present an alternative approach, in this way it might be possible to improve the dispersion and stability of the active metal sites without risking the formation of the inactive mixed metal oxide [10]. Materials based on activated carbon have been reported to be promising supports because they are relatively chemically inert [11-13]. Carbon provides a stable platform for the deposition of the active species [14] and carbon has been shown to enable the reduction of metal oxides in an inert atmosphere, as a result of auto-reduction [15]. To date there has been a growing trend for the use of activated carbon as a support for the FTS reaction [16-22].

In the present study we compare the catalytic activity of $CoMnO_x$ catalysts prepared by co-precipitation with $CoMnO_x$/carbon catalysts prepared by deposition precipitation. Furthermore, the effect of the heat treatment temperatures and the effect of the ageing time of the $CoMnO_x$/C precipitates on these catalyst materials have also been studied, since treatment temperatures and ageing times have been shown to effect catalytic activity and the product selectivity [23, 24].

2. Experimental

2.1.Catalyst preparation

2.1.1. Co-precipitation

$CoMnO_x$ catalysts were prepared according to the procedure given in the patent literature [19, 22, 25]. An aqueous solution was prepared containing equimolar amounts of cobalt nitrate hexahydrate ($Co(NO_3)_2 \cdot 6H_2O$, Sigma Aldrich, 99.999%) and manganese nitrate tetrahydrate ($Mn(NO_3)_2 \cdot 4H_2O$, Sigma Aldrich, $\geq$98%). This solution was heated to 80 °C and ammonium hydroxide (28-30% NH_3 in water, Sigma Aldrich) was added to raise the pH from 2.9 to 8.30 ±0.01. The resulting precipitate was recovered by filtration, washed with distilled water (1 dm^3, 80 °C), dried (110 °C, 16 h) and calcined in static air (500 °C, 24 h).

2.1.2. Deposition precipitation

$CoMnO_x$/C catalysts were prepared as according to the procedure given in the patent literature [19, 22, 25]. An aqueous solution was prepared containing equimolar amounts of cobalt nitrate hexahydrate ($Co(NO_3)_2 \cdot 6H_2O$, Sigma Aldrich, 99.999%) and manganese nitrate tetrahydrate ($Mn(NO_3)_2 \cdot 4H_2O$, Sigma Aldrich, $\geq$98%). Coconut shell-derived activated carbon (GCN3070, NORIT) was added to the mixed nitrate solution to give a final catalyst with a composition of 20% Co, 20% Mn and 60% activated carbon. The slurry was stirred for 10 min at 80 °C before ammonium hydroxide (28-30% NH_3 in H_2O, Sigma Aldrich) was added drop wise to the nitrate solution to raise the pH from 4 to 8.30 ±0.01. The resulting precipitate was recovered by filtration, washed with distilled water (1 L, 80 °C), dried (110 °C, 16 h) and heated in flowing He.

To study the effect of heat treatment, one batch of catalyst was divided into four portions which were heated in flowing He separately at 300, 400, 500, and 600 °C for 5 h.

To study the effect of ageing the precipitate was left in the mother liquor for the specific time intervals of 1, 2, and 3 h followed by heat treatment in He at 500 °C for 5 h.

2.2. Catalytic activity

The catalysts were pelleted and sieved (0.65-0.85 mm) and 0.5 g were loaded into stainless steel fixed bed reactors (internal diameter ¼"). Catalysts were reduced *in situ* at 400 °C for 16 h in pure hydrogen (GHSV = 600 h^{-1}) then cooled to room temperature and pressurized to 6 barg with syngas ($CO:H_2$ = 1:1 molar ratio). All catalysts were tested under identical reaction conditions, 240 °C, 6 barg, and GHSV = 600 h^{-1}.

A stabilization period of ~100 h was allowed before catalyst data was collected and the mass balance determined. Analysis of gas products was performed by on-line gas chromatography using a Varian GC-3800. Hydrocarbons were analysed using a CP-Al_2O_3/KCl column and a flame ionisation detector. Permanent gases and C_1-C_4 hydrocarbons were analysed using molecular sieve 13x and Poropak Q columns with TCD and FID detectors in series. Nitrogen was used as an internal standard. The product stream was cooled in a wax trap (~25 °C) to retain the liquid products. Calibrations were performed with standard samples (C_1-C_5 hydrocarbon mixture diluted with nitrogen, BOC certified) for data quantification.

2.3. Catalyst characterization

2.3.1. X-ray photoelectron spectroscopy (XPS)

XPS was performed using a Kratos Axis Ultra-DLD photoelectron spectrometer, using monochromatic Al kα radiation, at 144 W. High resolution and survey scans were performed at pass energies of 40 and 160 eV respectively. Spectra were calibrated to the C (1s) signal at 284.5 eV, which is typical for graphitic carbon as measured for HOPG, and quantified using CasaXPS v2.3.15, utilizing sensitivity factors supplied by the manufacturer.

2.3.2. Powder X-ray diffraction (XRD)

XRD measurements were performed using a Bruker AXS Company, D8 Advance diffractometer. Scans were taken with a 2θ step size of 0.02° and a counting time of 1.0 s

using Cu K_α radiation source generated at 40 kV and 30 mA. Specimens for XRD were prepared by compaction into a glass-backed aluminum sample holder. Data was collected over a 2θ range from 4° to 80° and phases identified by matching with the ICDD database.

3. Results and discussion

3.1. *Comparison of catalyst performance of $CoMnO_x$ and $CoMnO_x$/C catalysts*

The unaged catalysts were tested for the FTS reaction under identical conditions and the data are presented in Table 1. A comparison of the $CoMnO_x$ and $CoMnO_x$/C catalyst performance indicates the selectivity to carbon dioxide and methane was decreased markedly with the carbon-supported catalyst. CO conversion and the selectivity to C_{5+} hydrocarbons were higher compared with the pure $CoMnO_x$ catalyst. The effect of time-on-line is presented in Figure 1 and this shows that the carbon-supported catalyst attained steady state after 45 h, whereas the unsupported $CoMnO_x$ catalyst achieved steady state only after 90 h. Neither catalyst showed deactivation over the time period studied.

3.2. Effect of preparation variables on the performance of $CoMnO_x$ /C catalysts

3.2.1. Pre-treatment temperature

Pretreatment of the catalyst precursor, particularly the heat treatment temperature is a critical parameter in catalyst preparation which can affect the activity and selectivity of the supported catalysts [23]. In order to study the effect of the pretreatment, one batch of $CoMnO_x$/C was heated at different temperatures in He. CO conversion and product selectivity data are presented in Table 2 and it is apparent that there was a steady increase in CO conversion with increasing heat treatment temperatures from 300 to 500 °C. An increase in C_{5+} product selectivity was also observed together with a decrease in CO_2 selectivity. Previously, heat treatment studies of this type have been performed for oxide-supported Co catalysts [24, 26], but to date this has not been carried out for carbon-supported $CoMnO_x$ catalysts.

For the catalyst pretreated at 600 °C the CO conversion and the selectivity to CH_4 and CO_2 decreased markedly together with an increase in the selectivity of C_{5+} products. This

corresponds to a structural change which is evident from the XRD patterns (Figure 2). All catalysts showed the diffraction pattern for the mixed spinel oxide of Co and Mn (with an intermediate tetragonal structure between $CoMn_2O_4$ and Mn_3O_4) (ICDD 018-0408). The XRD pattern of the catalysts heated at 300 and 400 °C were found to be similar to each other, whilst an additional phase of Co metal was observed with a reflection at 41.9° (ICDD 15-0806) in the catalyst pretreated at 500 °C in addition to the mixed spinel oxide phases of $CoMn_2O_4$. The catalyst treated at 600°C displays the most significant change in the XRD pattern, with Co reflections at 36.0, 41.9 and 60.1° 2θ (ICDD 15-0806). This indicates that the Co nanoparticles are sintering and hence here is a loss in activity.

XPS derived molar concentrations are given in Table 3 and it is evident that there was no significant change in the Co:Mn molar ratios for heat treatments up to 500 °C, whereas the surface becomes Mn rich above this temperature. XPS core-level spectra in figure 3 show that with increasing treatment temperature the main Co($2p_{3/2}$) photoelectron signal remains consistent with Co^{2+} (*ca.* 780 eV). However, concomitant with increasing heating temperature is a steady change in the shake-up satellite structure above the main Co($2p_{3/2}$) photoemission line (indicated by an arrow in Figure 3a) which is consistent with the transformation of $CoMn_2O_4$ to CoO in the precursor.

Changes in the Mn spectra are more subtle, with a shift downward in binding energy of 0.5 eV between the samples prepared using heat treatment in He at 300 (641.9 eV) and 600 °C (641.4 eV). For the catalyst heated at 600 °C the Mn ($2p_{3/2}$) peak reveals some asymmetry to the lower binding energy side of the peak (indicated by an arrow, Figure 3b) suggesting the formation of MnO at the surface. XRD data (Figure 2) indicates that both $CoMn_2O_4$ and Co are present in the precursor for the sample heated at 600 °C, however, XPS analysis of the Co(2p) regions indicates the presence of CoO, which is attributed to Co being oxidized by exposure to air prior to analysis. This also explains the surface enrichment of Mn, and although CoO is also present at the surface, larger particles of CoO would give a lower apparent surface concentration. Clearly from the XRD and XPS analysis, the surface of this catalyst is different than the bulk. However, there is no segregation of MnO_x phases apparent in the XRD pattern, which indicates that the MnO_x phases are poorly crystalline.

3.2.2. Ageing time of the precipitates

Having explored the pretreatment temperature of the precursor, we next studied the influence of the ageing time of the precipitate during the catalyst preparation. Ageing of

precipitates for different time intervals has been found to be an important parameter in catalyst preparation [26]. Catalysts were prepared with a range of ageing times and then heated in He at 500 °C as this was observed to be the optimum treatment temperature. The activity data is provided in Table 4 and shows that the unaged catalyst exhibits lower selectivity to carbon dioxide and methane. Interestingly, there is a steady decrease in CO conversion and selectivity to C_{5+} hydrocarbons with an increase in ageing time of the precipitate. CO_2 selectivity also increased but the selectivity to CH_4 remained unchanged.

Previous studies on the effect of ageing time on cobalt oxide catalysts for various gas phase reactions [27, 28] have reported that the ageing of precipitates prepared by co-precipitation leads to phase changes towards thermodynamically stable materials. The phase analysis of the aged catalysts has been investigated by XRD and the data are shown in Figure 4. All materials exhibit the pattern for the mixed spinel oxide of Co and Mn with an intermediate tetragonal structure between $CoMn_2O_4$ and Mn_3O_4 (ICDD 018-0408). A Co phase was evident in the unaged catalyst from the reflection at 41.9° 2θ (ICDD 15-0806), but increased ageing times led to the formation of the cubic $CoMn_2O_4$ phase (ICDD 023-1237) and the Co was no longer apparent.

The XPS derived molar ratios or Co and Mn analysis are given in Table 5, whilst Figure 5 shows Co(2p) and Mn(2p) core-level spectra. For the unaged sample, the Co($2p_{3/2}$) peak at 780.2 eV is indicative of Co^{2+}, with an associated satellite structure at higher binding energy confirming the XRD evidence that CoO is present. The Mn($2p_{3/2}$) peak energy of 641.3 eV can be assigned to Mn_xO_y or $CoMn_2O_4$ and again this is in agreement with the XRD data. With increased aging time, both Co and Mn binding energies shift to slightly higher binding energy, consistent with the bulk $CoMn_2O_4$ [29]. There is an increase in amount of both metals on the surface of these catalysts with an increase in ageing time.

The Mn:Co molar ratios clearly show that the unaged catalyst exhibits a metal ratio close to unity as expected from the catalyst preparation, however, longer ageing times initially seem to decrease the apparent surface metal content, with a subsequent increase at higher ageing times which can be linked to the initial uptake of the metals in to the porous network of the carbon followed by further accumulation at the surface.

4. Conclusions

We have investigated and contrasted carbon-supported cobalt manganese oxide ($CoMnO_x$/C) catalysts and an unsupported $CoMnO_x$ catalyst for the FTS reaction. The carbon-supported catalyst gave increased catalyst activity and selectivity to C_{5+} hydrocarbons and the selectivity to CH_4 and CO_2 was decreased in comparison to the $CoMnO_x$ catalyst. In addition the carbon-supported catalysts attained a steady state performance far more rapidly than the unsupported catalyst. The effect of two key parameters; namely the heat treatment of the precursor prior to reduction and the effect of ageing of the initial precipitate have been studied and the optimal conditions identified. Most importantly ageing of the initial precipitate should be avoided to obtain good catalyst performance.

Acknowledgement

We are thankful to SABIC for financial support.

References

[1]. R. G. Copperthwaite, G. J. Hutchings, M. Van der Riet, J. Woodhouse, Ind. Eng. Chem. Res. 26 (1987) 869-874.

[2]. M. Van der Riet, G. J. Hutchings, R. G. Copperthwaite, J. Chem. Soc., Chem. Commun. (1986) 798-799.

[3]. M. Van der Riet, G. Copperthwaite, G. J. Hutchings, J. Chem. Soc., Faraday Trans. 83 (1987) 2963-2972.

[4]. F. M. Gottschalk, R. G. Copperthwaite, M. Van der Riet, G. J. Hutchings, Appl. Catal. 38 (1988) 103-108.

[5]. S. Colley, R. G. Copperthwaite, G. J. Hutchings, M. Van der Riet, Ind. Eng. Chem. Res. 27(1988) 1339-1344.

[6]. G. J. Hutchings, M. Van der Riet, R. Hunter, J. Chem. Soc. Faraday Trans. 85(1989) 2875-2890.

[7]. G. J. Hutchings, F. Gottschalk, R. Hunter, S. W. Orchard, J. Chem. Soc. Faraday Trans. 85(1989) 363-371.

[8]. S. E. Colley, R. G. Copperthwaite, G. J. Hutchings, S. P. Terblanche, M. M. Thackeray, Nature 339 (1989) 129-130.

[9]. M. A. Vannice, R. L. Garten, J. Catal. 56 (1979) 236-248.

[10]. N. E. Tsakoumis, M. Ronning, O. Borg, E. Rytter, A. Holmen, Catal. Today, 154 (2010), 162-182.

[11]. C. Park, M. A. Keane, J. Colloid Interface Sci. 266 (2003) 183-194.

[12]. J. A. Anderson, A. Athawale, F. E. Imrie, F. M. McKenna, A. McCue, D. Molyneux, K. Power, M. Shand, R. P. K. Wells, J. Catal. 270 (2010) 9-15.

[13]. G. L. Bezemer, P. B. Radstake, V. Koot, A. J. van Dillen, J. W. Geus, K. P. de Jong, J. Catal. 237 (2006) 291-302.

[14]. K.-S. Ha, G. Kwak, K.-W. Jun, J. Hwang, J. Lee, Chem. Commun. 49 *(*2013) 5141-5143.

[15]. H. Xiong, M. Moyo, M. K. Rayner, L. L. Jewell, D. G. Billing, N. J. Coville, ChemCatChem. 2 (2010) 514-518.

[16]. Y. Ding, H. Zhu, T. Wang, J. Tao, L.Y. Guiping, US20080293563A1, 2008.

[17]. H. Zhu, Y. Ding, Y. Lu, T. Wang, M. Jin, CN101318133A, 2008.

[18]. L. Shi, F. Chun, L. Xiao, CN103170637A, 2013.

[19]. K. Karim, M. Alsemahi, A. Khan, WO2014001354A1, 2014.

[20]. X. Sun, C. Hou, G. Xia, Y. Wu, M. Li, R. Xu, Z. Hu, H. Nie, CN103769235A, 2014.

[21]. L. Shi, Y. Wang, Y. Tan, CN103934040A, 2014.

[22]. K. Karim, G. Hutchings, S. Iqbal, WO2012143131A1, 2012.

[23]. B. Solsona, G. J. Hutchings, T. Garcia, S. H. Taylor, New J. Chem. 28 (2004) 708-711.

[24]. M. Feyzi, M. M. Khodaei, J. Shahmoradi, Fuel Processing Technology, 93 (2012), 90-98.

[25]. K. Karim, S. Al-sayaria, G. J. Hutchings, S. Iqbal, WO2014174374, 2014

[26]. M. Feyzi, M. Irandoust, A. A. Mirzaei, Fuel Processing Technology, 92 (2011) 1136-1143.

[27]. S. H. Taylor, C. Rhodes, Catal. Lett. 101 (2005) 31-33.

[28]. A. A. Mirzaei, M. Faizi, R. Habibpour, Appl. Catal. A 306 (2006) 98-107.

[29]. M. Oku, K. Hirokawa, J. Electron Spectrosc. Relat. Phenom. 8 (1976) 475-481.

Table and Figures

Table 1. Comparison of the catalytic activity of $CoMnO_x$ with $CoMnO_x$/C catalyst

	$CoMnO_x$	$CoMnO_x$/C
CO conversion (%)	36.0	48
	Product selectivity (%)	
CH_4	22.1	7.0
C_2	4.5	4.3
C_3	11.5	16.1
C_4	1.2	7.6
C_{5+}	17.0	43.4
CO_2	37.0	20.4
Alcohols	6.7	1.2

Reaction conditions: Catalyst 0.5 g, data collected at 115 h, 240 °C, 6 bar, CO:H_2 1:1 mol ratio,GHSV 600 h^{-1}

Table 2. Effect of heat treatment during preparation of $CoMnO_x$/C catalysts

Heat treatment temperature (°C)	**300**	**400**	**500**	**600**
CO conversion (%)	41.2	47.0	48.9	18.1
		Product selectivity (%)		
CH_4	15.1	16.9	8.4	1.3
C_2	8.3	5.3	5.6	1.7
C_3	23.2	20	17.1	6.3
C_4	3.2	3.6	7.0	1.1
C_{5+}	22.7	26.3	41.4	89.6
CO_2	13.5	15.1	19.4	0
Alcohols	14.1	12.8	1.2	0

Reaction conditions: Catalyst 0.5g, 240 ^oC, data collected at 146 h, 6 bar, CO:H_2 1:1 mol ratio, GHSV 600 h^{-1}

Table 3. XPS derived molar concentrations for each preparation temperature

Heat treatment Temperature	**Molar composition (%)**				**Ratios**
	O	C	Co	Mn	Mn/Co
300 °C	38.7	36.5	12.4	12.5	1.01
400 °C	43.5	27.7	15.0	13.8	0.92
500 °C	43.3	27.8	14.1	14.8	1.05
600 °C	39.5	34.7	8.1	17.7	2.19

Table 4. Effect of ageing time of the precipitate on the activity and selectivity of $CoMnO_x$/C catalysts

	0h	**1h**	**2h**	**3h**
CO conversion (%)	48.9	36.8	29.6	27
	Product selectivity (%)			
CH_4	8.4	8.3	8.9	9.2
C_2	5.6	4.4	4.8	6.0
C_3	17.1	17.5	14.5	16.7
C_4	7.0	5.1	5.6	5.7
C_{5+}	41.4	40.0	35.0	25.0
CO_2	19.4	23.0	29.0	38.0
Alcohols	1.2	2.0	3.0	0.0

Reaction conditions: Catalyst 0.5 g, 240 ^oC, data collected at 140 h, 6 Barg, CO:H_2 1:1 mol ratio, GHSV 600 h^{-1}

Table 5. XPS derived molar surface concentrations for Co/Mo/C aged for different times

Ageing Time	**Molar composition (%)**			**Ratio**	
	O	C	Co	Mn	Mn/Co
0 h	43.3	27.8	14.1	14.8	1.05
1 h	15.6	76.9	3.0	4.4	1.45
2 h	18.8	69.3	5.6	6.4	1.15
3 h	22.8	61.7	7.1	8.5	1.20

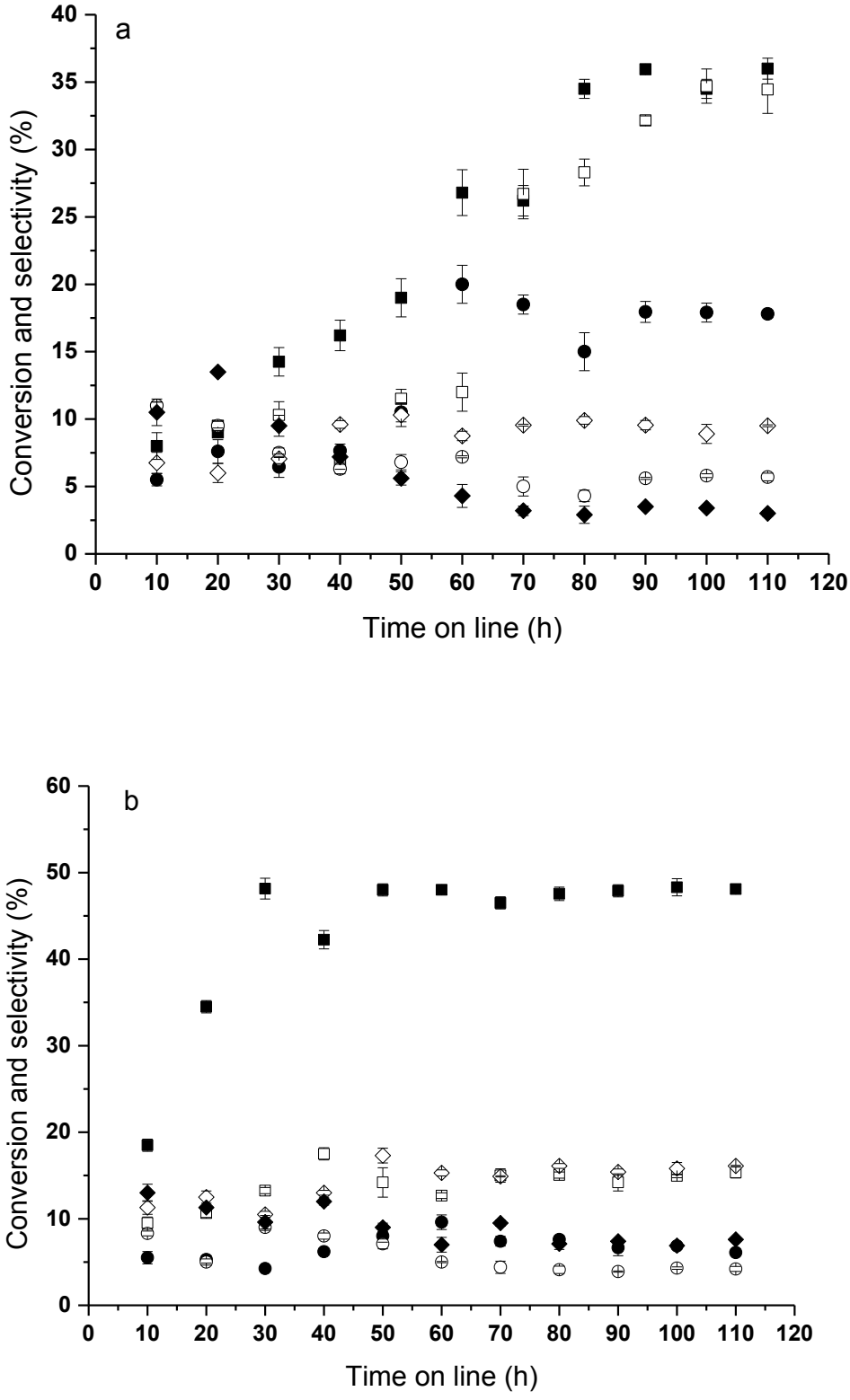

Figure 1. Time on line study on a) $CoMnO_x$ catalyst b) $CoMnO_x$/C catalyst.

■ CO conversion, □ CO_2, ● CH_4, ○ C_2,◊ C_3, ♦ C_4 Error bars are shown, if not visible the error is equivalent in scale to the symbol.

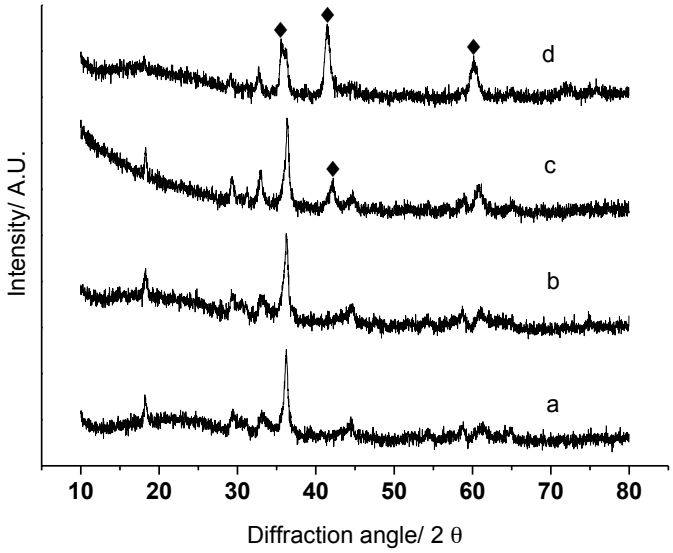

Figure 2. Powder X-ray diffraction pattern for Co/Mn/C catalysts heated at different temperatures; a. 300 °C, b. 400 °C, c. 500 °C, d. 600 °C. ♦ Co

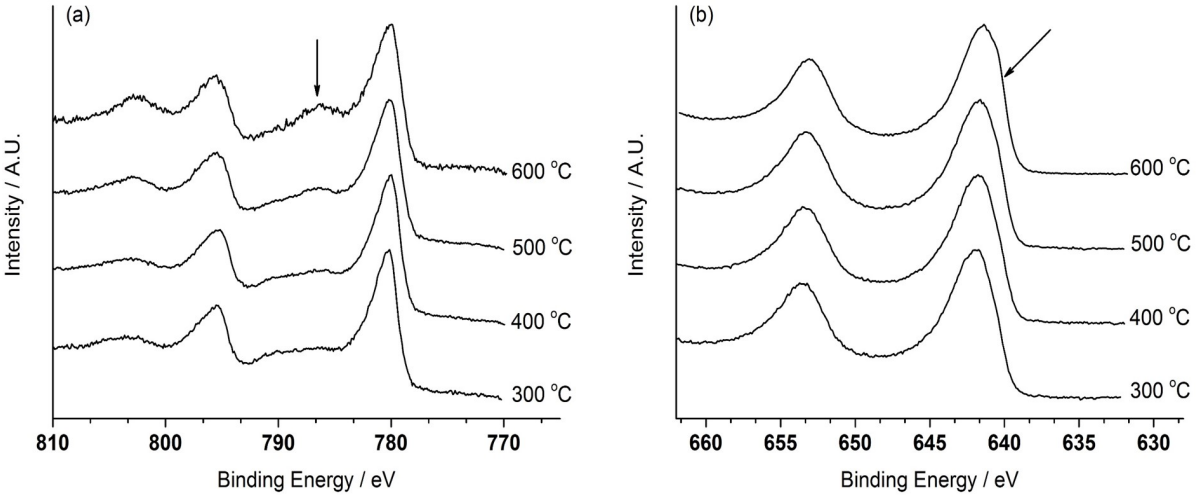

Figure 3. X-ray photoelectron core-level spectra for Co/Mn/C catalysts treated at different temperatures; a) Co(2p) and b) Mn(2p)

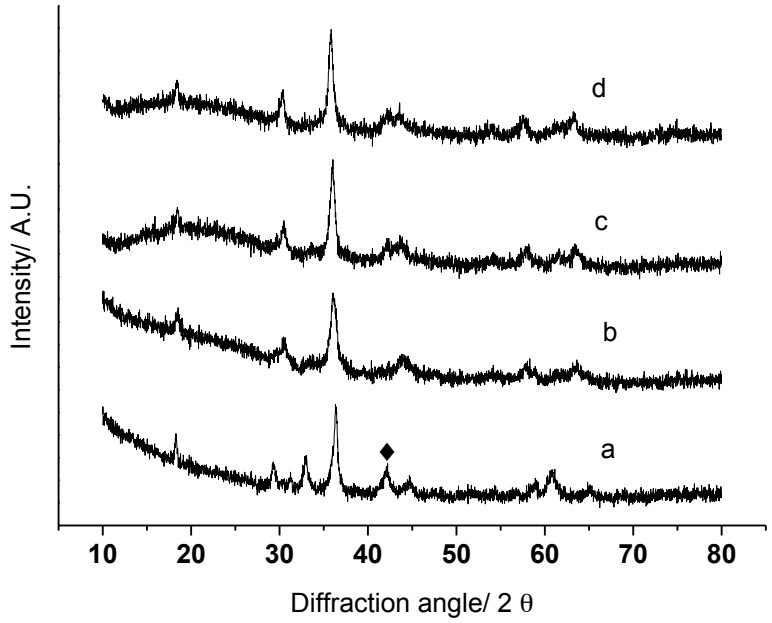

Figure 4. Powder X-ray diffraction pattern for Co/Mn/C catalysts prepared with different ageing times of a) Unaged, b) 1 h, c) 2 h and d) 3 h ♦= Co

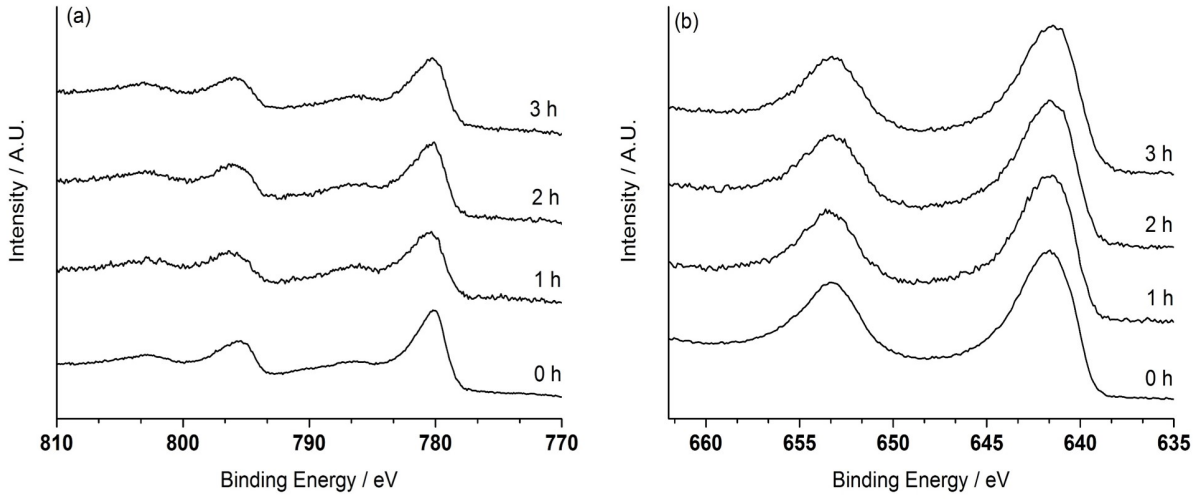

Figure 5. X-ray photoelectron core-level spectra for Co/Mn/C catalysts with different aging times; a) Co(2p) and b) Mn(2p)